Degradation of Chlorinated Organics by Membrane-Immobilized Nanosized Metals

D.E. Meyer,[a] K. Wood,[a] L.G. Bachas,[b] and D. Bhattacharyya[a]

[a] Dept. of Chemical and Materials Engineering, University of Kentucky, Lexington, KY 40506-0046; db@engr.uky.edu (for correspondence)

[b] Dept. of Chemistry, University of Kentucky, Lexington, KY 40506-0046

Published online in Wiley InterScience (www.interscience.wiley.com). DOI 10.1002/ep.10031

The use of electronegative metals, such as Fe, has been extensively studied for the treatment of groundwater containing toxic chlorinated organics. Much of the recent work has been focused on the use of nanoscale particles with diameters from 2 to 100 nm. This work examines the use of bimetallic (Fe/Ni) nanoscale particles immobilized in a cellulose acetate domain for the destruction of trichloroethylene (TCE). The organic/inorganic hybrid film is synthesized using phase inversion with sodium borohydride reduction. The resulting nanoparticles have an average diameter of 24 nm. Using a small quantity of membrane-immobilized metal (31 mg total, Fe:Ni = 4:1), it was possible to achieve over a 75% reduction in TCE levels in 4.25 h, with ethane as the only observable product. For shorter reaction times (<2 h), traces of cis- and trans-DCE could be extracted from the baseline of the MS chromatogram. For longer reaction times, products of coupling reactions (butane and hexane) were observed. This corresponds to a surface-area–normalized pseudo–first-order rate constant, k_{SA}, for the immobilized system of 3.7×10^{-2} L m^{-2} h^{-1}. Analysis of the aqueous phase for metal content showed minimal leaching of the metals into the surrounding solution during treatment. Because various combinations of membranes containing immobilized metal nanoparticles can be achieved using the synthesis techniques presented, a more versatile platform for the application of zero-valent treatment is possible. © 2004 American Institute of Chemical Engineers Environ Prog, 23: 232–242, 2004

Keywords: metal nanoparticles, Fe/Ni, synthesis, cellulose acetate membrane, dechlorination, TCE, DCE

INTRODUCTION

Hazardous organics degradation/dechlorination from dilute solutions has been reported extensively for both oxidative and reductive processes. Room-temperature oxidation processes include ozone, ozone + hydrogen peroxide, Fenton's reaction, and so forth, whereas reductive processes include various zero-valent metals, such as Fe, Zn, Fe/Pd, and the like. The main difference between oxidative and reductive processes is complete reaction in the former leads to the formation of CO_2, whereas the latter results in formation of the nonchlorinated analog of the parent compound [for example, ethylene/ethane from trichloroethylene (TCE)].

Kinetics of Dehalogenation and the Impact of Metal Surface Area

Since the original work of Gillham and O'Hannesin [1] demonstrating the ability to reduce toxic chlorinated compounds using zero-valent metal, a large effort has been made to both fundamentally understand the kinetics of these systems and dramatically enhance the rate of reaction [2–13]. The most widely studied compound in the literature is TCE because of its importance in groundwater remediation. The destruction of TCE with Fe is an electrochemical corrosion process involving the following half reactions:

$$3Fe^0 \rightarrow 3Fe^{2+} + 6e^- \quad (1a)$$

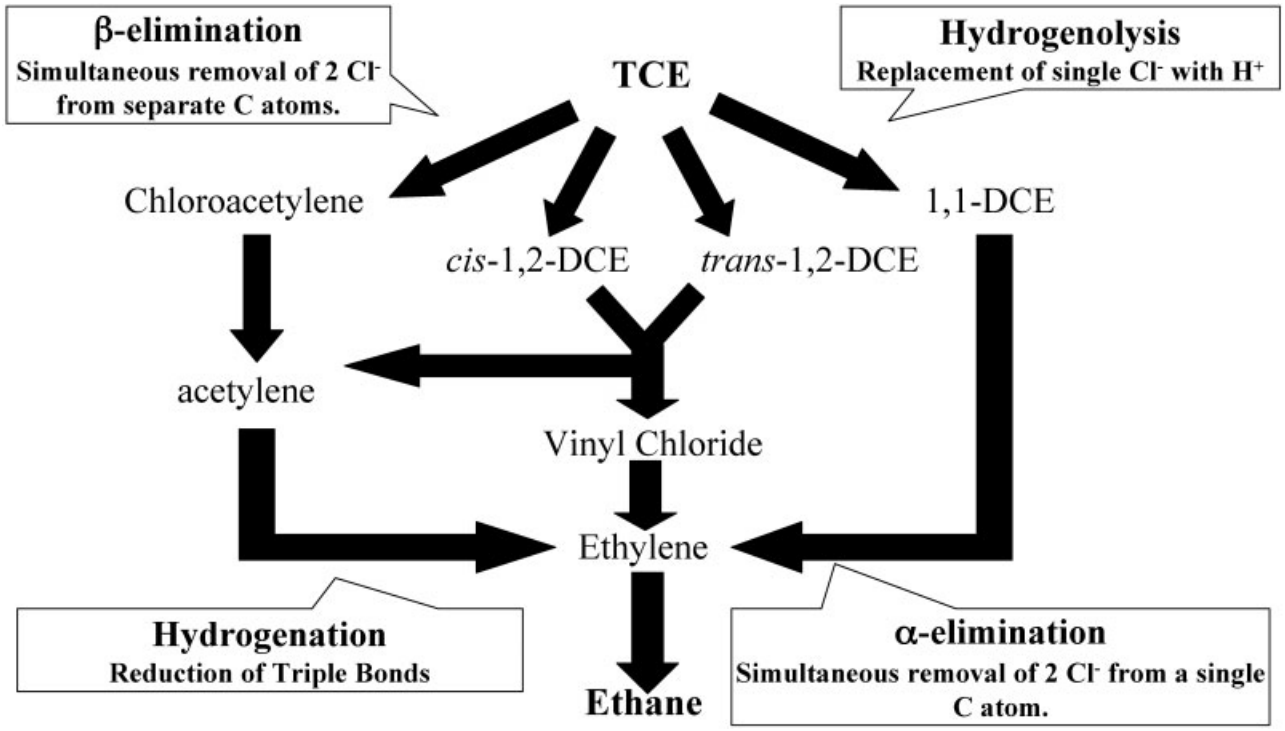

Figure 1. Complex reaction mechanism associated with the reductive dechlorination of trichloroethylene (TCE) using zero-valent Fe. Adapted from Arnold and Roberts [4].

$$CCl_2CHCl + 3H^+ + 6e^- \rightarrow C_2H_4 + 3Cl^- \quad (1b)$$

Studies by Arnold and Roberts to determine the kinetic mechanism of this system established several competitive pathways involving various intermediates, some of which (such as vinyl chloride) are more toxic than the parent compound [4]. A possible overall reaction scheme for this system is shown in Figure 1. Because the reactions take place on the iron surface, it is important that knowledge of the adsorption behavior of TCE and its intermediates be understood when modeling the kinetics of the system [4, 8, 11]. Many researchers have found that unfavorable side reactions involving iron and dissolved oxygen, water, or inorganics such as nitrate are known to occur, which thus adds to the complexity of the system. It has been shown that the incorporation of a second coating metal, such as nickel or Pd, allows for the protection of the Fe layer from oxidation with the added enhancement of catalytic activity through hydrogenation [14, 15].

Early results for dechlorination of TCE by Fe in the literature are representative of the key problems associated with this system. Mainly, the reaction time required for complete degradation of the parent compound by bulk Fe is on the order of days [2, 4, 10]. Within these results, the actual reaction time required depends largely on the quantity of Fe surface area used in the system [11, 16]. Most kinetic models for these results have been developed for the reaction of the parent compound and suggest a pseudo–first-order behavior in this case:

$$\frac{dC_w}{dt} = -kC_w \quad (2)$$

where k is the observed pseudo–first-order rate constant (h^{-1}) and C_w is the aqueous phase concentration of TCE (typically mg L^{-1}). An in-depth treatment of the pseudo–first-order model can be found in the work of Tratnyek and co-workers [2]. The most significant impact of their work is the introduction of a surface-area–normalized rate constant (k_{SA}, L m^{-2} h^{-1}) to allow comparison of the various results. For this parameter, the reaction rate constant is normalized using the metal (in this case Fe) surface area loading as follows:

$$k_{SA} = \frac{k}{a_s \rho_m} \quad (3)$$

where a_s is the Fe surface area (m^2 g^{-1}) and ρ_m is the amount of Fe in solution (g L^{-1}). Analysis of this parameter from various researchers still shows variations in reported rate constants and suggests that factors other than surface area loading have significant impact on the kinetics of the system [2].

The desire to control the wide variability of results and reduce reaction time has caused researchers to turn their attention to the role of surface area and surface interactions. For example, pitting of the metal surface with acid pretreatment has been reported to help remove oxide layers forming at the iron surface, providing more available surface area, or more specifically,

more reactive sites [16]. The effectiveness of this type of pretreatment was questioned by Su and Puls [8] because they found that the calculated k_{SA} values for their pretreatment experiments were lower than values for untreated cases. However, they did point out that this might be attributed to impurities in the metal matrix that would not contribute to an increase in reactive sites when exposed by acid treatment. The surface chemistry of the metal also affects the rates of degradation as increased oxide layer growth leads to increased diffusional resistance for electron transfer. In addition, the role of natural organic matter (NOM) was found to be important for the dechlorination of certain organics (CCl_4, TCE) by Fe [13].

Improvements to Dechlorination Systems

Current trends in zero-valent metal dechlorination systems involve the use of nanoscale metals, which possess much more surface area per unit mass than bulk-scale material. Studies involving these particles have increased reaction rates by several orders of magnitude. In particular, the work of Zhang and coworkers [7, 14, 17–19] has demonstrated the ability of both Fe and bimetallic (that is, Fe/Pd) nanoparticle systems to detoxify a wide range of compounds [TCE, perchloroethylene (PCE), PCBs, etc.] in only a matter of hours. A detailed account of their system's performance, including *in situ* field assessment, has been given in the literature [17].

Solute Partitioning in Membrane Systems

Further improvement to reaction kinetics is believed possible by incorporation of a polymeric phase, or membrane containing the zero-valent metal. The reasoning for this is that it provides two key advantages over traditional aqueous-phase systems. One advantage lies within the ability of the polymer to allow controlled growth of the zero-valent metal nanoparticles, which will be discussed more in-depth in the discussion of synthesis techniques for nanoparticle systems. The other advantage is related to local organic concentration around the metal nanoparticles. Selective partitioning by the organic should result in a higher localized concentration of organic (such as TCE) in the membrane domain and provide a significant enhancement of reaction rates. In addition, a polymer phase will minimize the adsorption of undesired species, such as bacteria, on the particle surface. The concept of supported nanoparticles for the remediation of aqueous metal contaminants in groundwater has been presented by Mallouk and co-workers [20] in the literature. Their work focused on the use of hydrophobic resin supports that were intended to both decrease nanoparticle agglomeration during synthesis and increase the available reactive metal surface area for groundwater treatment.

It is important to address the possible impact of the polymer, when modeling the reaction kinetics. It must be noted that the observed reaction rate constant for this type of system is a function of several key factors: $k = f$(*particle surface area, temperature, pH, membrane sorption and diffusion*).

The pseudo–first-order model (Eq. 2) used to describe the kinetics is based on the aqueous phase concentration of TCE and does not account for mass transfer of TCE to the particle surface. In solution phase with sufficient mixing, resistance to external mass transfer can be considered negligible. On the other hand, migration of TCE through the membrane domain in the absence of convection may have significant impact on the ability of the diffusing species to reach the particle surface for reaction, depending on the hydrophobicity of the membrane. This effect will influence the observed reaction kinetics.

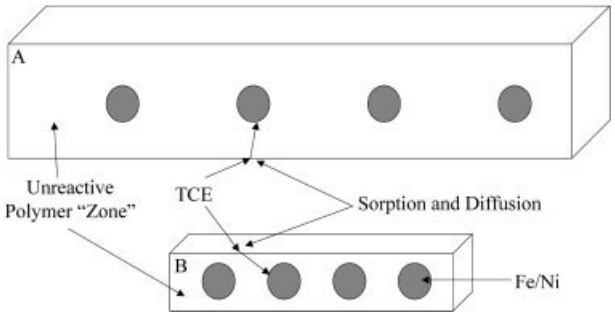

Figure 2. Schematic of TCE sorption and diffusion into a reactive membrane showing the greater volume of "unreactive polymer" zone that must be traveled for membranes containing the same mass of metal nanoparticles. The membranes are identical, except that membrane A has half the particle-surface-area-to-membrane-volume fraction of membrane B and will therefore have slower observed kinetics if mobility of TCE within the polymer is limited.

The degree to which this mass transfer limitation becomes a problem will largely depend on the ratio of particle surface area (m^2) to membrane volume (m^3). The larger this ratio, the less "unreactive polymer" zones separating the particles. Given that sorption of TCE occurs throughout the entire interface of the membrane domain with the adjacent solution, the TCE must diffuse through the "unreactive polymer" zones to reach the particle surface; thus the observed reaction rate will be slower for membranes with smaller surface-area-to-volume ratios. The magnitude of this effect will also depend on both the solubility and diffusivity of TCE in the membrane polymer. An illustration of this phenomenon is given in Figure 2.

Formation of Metal Nanoparticle Systems

A great deal of attention has been given to understanding the synthesis of nanoparticles. The majority of these techniques can be classified into two general types: (1) formation within solutions, and (2) formation within polymeric matrices. Nanoparticle formation within solution is probably the more common of the two classes of formation processes. The most frequently used method is the direct reduction of metal ions from solution using a reducing agent such as sodium borohydride ($Fe(H_2O)_6^{3+} + 3BH_4^- + 3H_2O \rightarrow Fe^0 + 3B(OH)_3 + 10.5H_2$, [3]). Glavee and coworkers [21] initially presented the method for zero-valent iron in 1995. Zhang *et al.* [7] later modified the procedure to

overcome the need for an inert atmosphere. The resulting particles typically have a broad range of particle size (often 1–100 nm). Other methods of synthesis include surfactant-mediated techniques, usually using micellar "nanoreactors" to control particle size [22–24]. These methods usually require extensive washing to remove the surfactant from the system and can often result in particle agglomeration in the absence of the surfactant, if no support is used to capture the nanoparticles.

Membrane-Directed Nanoparticle Synthesis

The present work will focus on the use of polymeric matrices for nanoparticle formation. The main advantage of polymer-based techniques is the enhanced ability to control the size distribution of the resulting nanoparticles. Through functionalization or variations in casting compositions and conditions, polymeric matrices can be assembled in a way that provides a template for nanoparticle growth as a result of steric hindrance within the matrix [25].

A typical method of formation involves thermolysis of organometallic compounds within a polymer film to produce the reduced metal nanoparticles [26]. A more tedious alternative to this approach is the use of diblock copolymers to create highly ordered nanodomains within a thin film. Hashimoto and co-workers [27, 28] were able to use this method to create organic/inorganic hybrid thin films containing either Ni-coated channels or 4-nm Pd^0 particles with little variation in particle size.

The present work examines the possible use of the more conventional and much simpler phase-inversion membrane preparation technique to incorporate metallic nanoparticles into a thin film. During the phase-inversion process, a polymer is dissolved in an appropriate solvent. The addition of a second solvent (antisolvent) that is insoluble to the polymer will induce nucleation of the polymer phase. In this way the polymer "inverts," or demixes from the solvent phase to form a polymer-rich phase. For preparation of thin films, the homogeneous polymer solution can be cast onto a flat surface and then immersed into a coagulation bath containing an appropriate antisolvent. The morphology of the resulting film can be controlled based on cast composition and environmental factors (such as temperature, humidity, etc.), which will determine whether the demixing process is rapid or delayed. For more dense structures (which should allow for smaller particle size), delayed demixing is preferred.

The main hypothesis behind our work is that nanosized Fe or Fe/Ni particles of <50 nm can be synthesized in a polymer (membrane) domain and used for treatment of chlorinated compounds. Membrane immobilization should lead to enhanced organic degradation rates with lower metal loadings attributed to surface area effects, particle reactivity, and membrane partitioning of the organic pollutant. The objectives of this work are (1) formation of nano-sized metallic (mainly Fe/Ni) particles in commonly used membrane material, (2) establishment of TCE degradation kinetics, and (3) comparison of our rate results with solution-phase literature data. Although conventional membranes (such as dense reverse osmosis and nanofiltration membranes) are primarily used for separation of salts and organics [29, 30], the incorporation of nanosized metals provides simultaneous separation and organic destruction opportunities at room temperature.

EXPERIMENTAL PROCEDURES

Cellulose acetate (CA) was selected for the membrane polymer over more hydrophobic polymers, primarily because fabrication of the membrane using the phase-inversion technique is well established in the literature. In addition, water can be added to the cast solution, allowing metal salts to be easily incorporated in the aqueous domain. The procedure given below is for the formation of a Fe/Ni bimetallic system. However this procedure could easily be extended to any desired metal that can be solubilized in an aqueous medium. The model compounds studied in this work are TCE, *cis*-1,2-dichloroethene (DCE), and 1,1,2,2-tetrachloroethane (TtCA). TtCA was chosen because of its low volatility at room temperature and availability of literature data for bulk-scale particle dechlorination. TCE and its intermediate DCE were selected because of the high priority of TCE in groundwater remediation and abundance of literature results for both bulk-scale and nanoscale dechlorination. (See Table 1 for a summary of experimental conditions and results.)

Materials

$FeCl_2 \cdot 4H_2O$ (crystalline, reagent, Fisher) and $NiCl_2 \cdot 6H_2O$ (Baker, reagent, 99.6%) were obtained and used as sources of Fe/Ni in the bimetallic nanoparticle synthesis. Cellulose acetate (Lot #A17A, acetyl content = 39.4%) was obtained from Kodak to be used as the membrane. $NaBH_4$ (Aldrich, granules, 99.995%) was used as the reducing agent for all cases. TCE (Aldrich, 99.9%, A.C.S.), *cis*-1,2-DCE (Aldrich, 99%), and TtCA (Aldrich, 98%) were obtained and used in dechlorination studies without further purification. Acetone (99.5%, A.C.S.), pentane (Aldrich, 99%, spectrophotometric), 1,2-dibromoethane (EDB) (Aldrich, 99%), and sodium nitrate (aq) were acquired for use in analytical techniques. All water used in the experiments was deionized ultrafiltered (DIUF) water (Fisher).

Membrane Preparation

Membranes were obtained by first preparing a 0.3 M Fe^{2+}/0.075 M Ni^{2+} solution (4:1, Fe:Ni) using $FeCl_2 \cdot 6H_2O$ and $NiCl_2 \cdot 6H_2O$, and allowing it to mix until the metal salts were completely dissolved. This solution was then added to a casting solution containing cellulose acetate dissolved in acetone until the final composition by weight of the casting solution was 18.03% cellulose acetate, 14.72% water, 0.88% $FeCl_2$, 0.03% $NiCl_2$, and 66.34% acetone. This composition was selected based on the classical procedures for preparing dense reverse-osmosis membranes presented by Sourirajan and Matsaura [31]. Modifications were made to allow for larger metal loading in the membrane. The solution was mixed and allowed to sit at 4° C until the presence of gas bubbles could not be

Table 1. Summary of experimental conditions and results for TCE, DCE, and TtCA dechlorination studies involving membrane-immobilized Fe/Ni (4:1 metal ratio).*

	Reaction time (h)	Fe^0/Ni^0 (mg L^{-1})	Parent compound $C_w/C_{w,0}$	k_{SA} (L m^{-2} h^{-1})
TCE				
($C_{w,0}$ = 9 mg L^{-1})	0.75	282	0.78	
	2	282	0.39–0.42	
	3.17	282	0.32	3.7E-02
	4.25	282	0.23–0.27	
cis-1,2-DCE				
($C_{w,0}$ = 5 mg L^{-1})	0.75	290	0.18	
	1	290	0.09	
TtCA				
($C_{w,0}$ = 12 mg L^{-1})	2.5	254	0.51	
	16	254	0.01	

*For all cases, initial pH = 4.0 and reactor volume = 110 mL.

visibly detected. A film was cast on a glass plate at room temperature (21° C) using a Gardner's® knife set at 14 mils. Initial solvent evaporation was allowed to proceed for 30 s to allow formation of a skin layer on the surface of the polymer film.

Formation of Metal Nanoparticles

The glass plate was then immediately immersed in a chilled coagulation bath containing 0.02 M $NaBH_4$ in water at a temperature of 1° C. The film was soaked for 15 min to allow complete demixing of the polymer solution with simultaneous particle formation. Excess $NaBH_4$ was used to help prevent oxidation of the metal particles after formation. Upon removal, the membrane was dried and rinsed twice with 500-mL portions of water. The first wash was at pH 2 to induce rapid reaction of residual $NaBH_4$ with water. The second wash was performed at pH 6.2 to equilibriate the membrane with the optimal pH for dechlorination studies. Samples were taken of the coagulation bath to determine metal loss during synthesis. A sample of the reduced membrane was saved in ethanol for particle imaging.

Dechlorination Studies

Two 120-mL glass bottles capped with Mininert® (Supelco) valves were filled with 110 mL of a chlorinated organic solution at pH 4, allowing for a 10-mL headspace. The chlorinated organic solutions were made using DIUF water that had been deoxygenated by bubbling nitrogen (99.995%, research grade) through it for 1 h. The initial pH was intentionally set lower (pH 4 vs. pH 6.2) to counteract any pH effects of residual $NaBH_4$, which would cause a pH shift to 8–10. This basic pH range has been shown in literature to cause a decrease in dechlorination rates [32]. The reduced membrane was cut into strips and placed in one of the glass bottles. The second glass bottle was used as a volatility control. Both bottles were placed on a wrist-action shaker and mixed throughout the duration of the experiment.

At the desired reaction interval, a known volume of headspace was withdrawn using a gas-tight syringe and directly analyzed using GC/MS. Immediately after the headspace was sampled, 2.5-mL aqueous samples (two total) were withdrawn and injected into 39.5 mL of DIUF water to dilute the samples for analysis by purge-and-trap (PT) GC/MS. An additional 15 mL of the aqueous phase was withdrawn to analyze the pH and metal content. The last step of sampling involved extraction of the membrane-phase organics into pentane for analysis by GC/MS. In this case, 20 mL of pentane containing 200 mg L^{-1} EDB was added back to the reactor. The reactor was placed back on the shakers for 15 min and then allowed to sit and equilibrate for an additional 5 min. A 1-μL aliquot was removed by syringe and analyzed by GC/MS.

Analytical Techniques

Organic analysis was performed using a Hewlett–Packard 5890 Series II gas chromatograph equipped with a Series 6150 mass spectrometer. For the bimetallic experiments, an OI Analytical Model 4560 Purge-and-Trap was coupled to the GC/MS and used for direct analysis of the aqueous phase. A 12–15% error in analysis was observed over an extracted organic concentration from 75 to 300 mg L^{-1}. For PT-GC/MS, the associated error was determined to be 15 to 20% based on feed analysis. For example, for a known feed of 11.7 mg L^{-1}, organic analysis typically yielded a concentration of about 9 mg L^{-1}. However, theoretical calculations do not take into account vapor-phase partitioning of the feed in the volumetric flask. In addition to unknown samples, periodic known samples were analyzed following the same procedure to ensure proper operation of the equipment. Samples to determine pH were analyzed using an Accumet dual-electrode meter and AccuTupH double-junction silver/silver chloride pH electrode. For the preliminary Fe^0/CA studies mentioned below, the amount of Cl^- in each sample was determined using an Orion Model 9617BN combination ion-selective electrode, manually calibrated for a working range of 1–50 mg L^{-1}, with a standard devia-

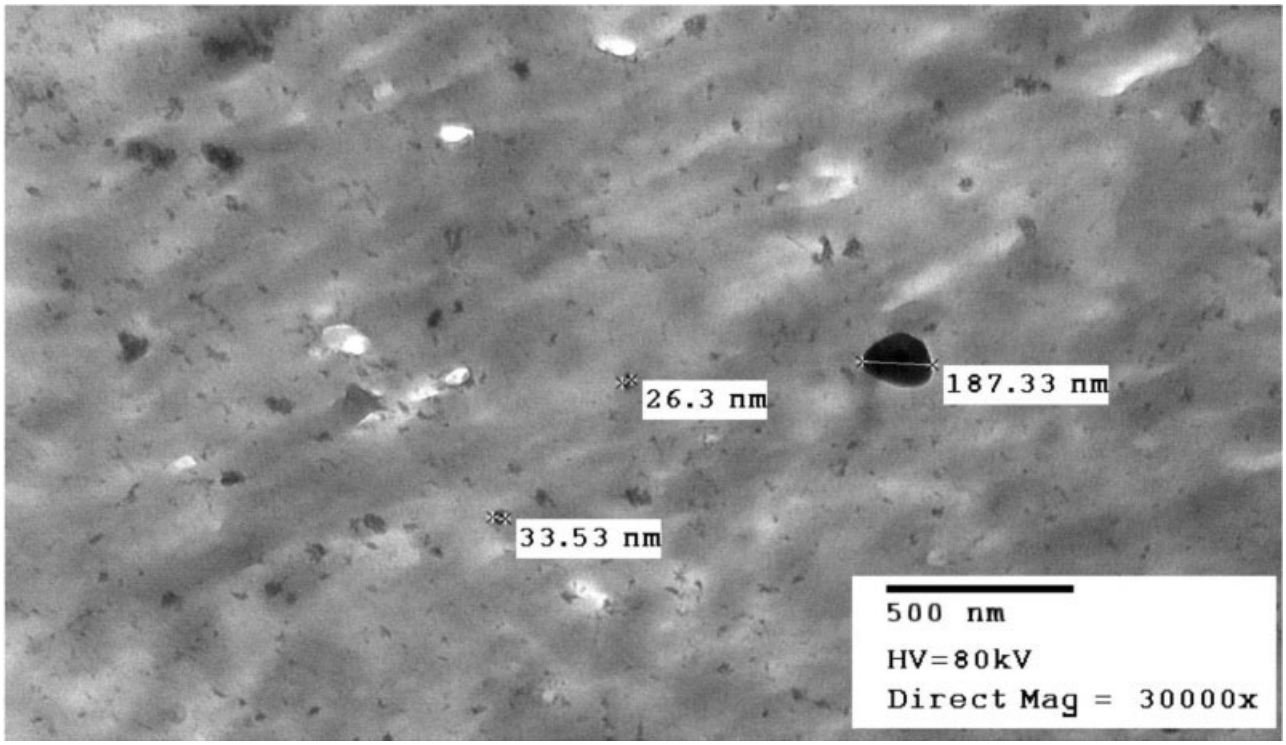

Figure 3. TEM image of the cross section of an Fe/cellulose acetate mixed-matrix membrane prepared by phase inversion showing particle size and distribution in skin region. The typical particle size was around 25 nm.

tion in millivolt response from 0.2 to 0.5 mV. The standard addition method was used to check results.

For samples to calculate metal loss during membrane synthesis, the amount of Fe and Ni was determined using a Varian SpectrAA 220 Fast Sequential atomic absorption spectrometer equipped with Fisher Scientific data-coded hollow cathode lamps. The sensitivity of the instrument permits linear analysis up to 5 mg L^{-1} with up to a 3.3% error for Fe and up to 3 mg L^{-1} with a 2% error for Ni.

Particle size was determined using either a Phillips Tecnai 12 TEM operating with an 80-kV source (Fe systems) or a JEOL 2010 field emission TEM operating with a 200-kV source (Fe/Ni systems). Both scopes are equipped with energy-dispersive X-ray (EDX) and a digital camera. EDX provided the verification of Fe/Ni presence in the membranes. For all cases, samples both with and without osmium coating were dried overnight at 50° C and embedded in Spurr's resin for 48 h at 60° C. A cross section of the membrane was cut and mounted on a copper grid. The digital camera was used to take photographs of the membrane, which could then be used to determine an average particle size.

RESULTS AND DISCUSSION

The following discussion of results is presented in two parts: (1) Fe nanoparticles and (2) Fe/Ni bimetallic nanoparticles in cellulose acetate membrane domain. In addition to volatility controls, blank experiments using membranes with no metal were performed to ensure the accuracy of the analytical procedures used to account for sorption of the parent compound by the membrane. Results from these experiments show a complete recovery for all organic compounds tested. For the case of Fe, results include Cl^- analysis because the source of Fe used ($FeNO_3$) did not contain Cl^-. However, recent work has shown that the presence of nitrate in dechlorination systems can greatly suppress reaction rates and led to the use of Cl^--based salts for the synthesis of the Fe/Ni system [33]. For all cases, the primary data used to evaluate system performance constituted the change in parent compound levels within the reactor. Although data concerning pH are not presented, in most cases the final pH shifted to a range of 8.5–10, indicating the presence of residual $NaBH_4$ that had been washed out from the membrane.

Preliminary Studies: Fe and TtCA

Before examining bimetallic systems, cellulose acetate films containing 25- to 200-nm Fe particles were synthesized using the techniques outlined above. Although particles as large as 200 nm were observed, there was a much narrower distribution of particle sizes, with a typical diameter of 25 nm. A representative TEM image of the cross section of these films is shown in Figure 3. The films were used in dechlorination studies of TtCA. Up to 70% reduction in TtCA levels was observed in 2 h using about 8.5 mg of Fe, which corresponds to an 18% dechlorination. The Cl^- data for this case indicated that only a 14% dechlorination had occurred. The formation of TCE as an intermediate was confirmed by GC/MS analysis for five of the trials. For the data given above, the amount of TCE present is 15%

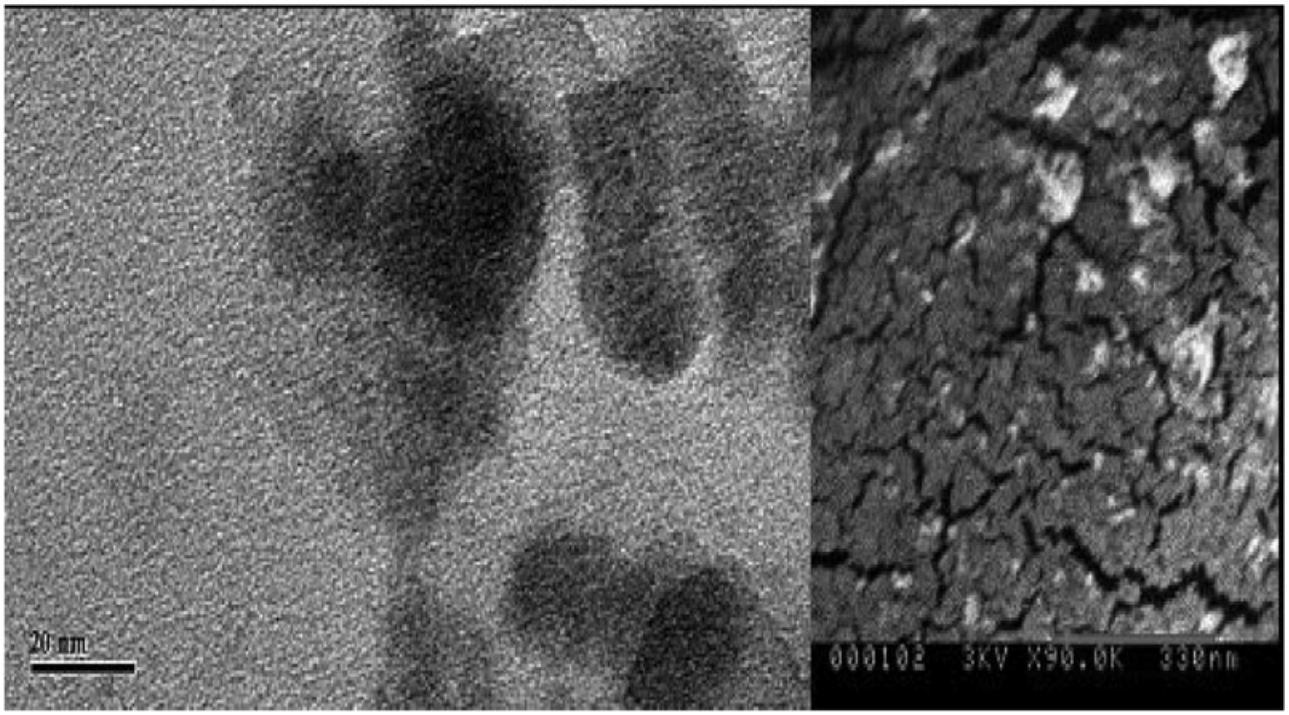

Figure 4. TEM (left) and SEM (right) images of Fe/Ni bimetallic nanoparticles synthesized in a cellulose acetate film. The typical particle size, both at the surface and in the cross section, is 24 nm. [Color figure can be viewed in the online issue, which is available at www.interscience.wiley.com.]

of the maximum value possible, based on TtCA converting only to TCE during dehalogenation.

The observed abundance of TCE is inconsistent with the reductive mechanism for TtCA proposed by Arnold *et al.* [34], which identified *cis*- and *trans*-DCE as the primary reductive products. Examination of the pH showed that in some cases the pH shifted into a range of 9–11, which indicates the presence of excess $NaBH_4$. For this pH range, it is possible that the actual organic destruction was the result of a combination of dehydrochlorination (loss of HCl from hydrolysis) and reductive elimination. Arnold *et al.* [34] did observe a higher production of TCE than hypothesized. It is therefore possible that the immobilized Fe acts to catalyze the reaction pathway to TCE. Further studies in this area are needed to better understand our observed TCE production.

These preliminary experiments involved an "evolving headspace," given that multiple samples were taken from the same reactor. This methodology was used because substantial oxidation occurred during synthesis, resulting in a wide variability of results. Additional corrections for partitioning into the vapor and membrane phases thus had to be made. The variability of the results is what ultimately led to the use of a second "protective" metal to help prevent the onset of oxidation. In addition, refinements to the synthesis techniques were also made to reduce the levels of residual $NaBH_4$ and the amount of time the membrane was in contact with air.

Membrane-Immobilized Fe/Ni Bimetallics

The films obtained using phase inversion were approximately 25 × 24 cm with a thickness of 115 μm. The films contained 31 mg of metal particles (24.8 mg Fe, 6.2 mg Ni), which is approximately 2% by weight. The films had a permeability of approximately 3×10^{-7} cm s^{-1} bar^{-1}. Results from TEM analysis of the membranes are shown in Figure 4. The membrane-immobilized bimetallic particles had an average diameter (population size = 75 particles) of 24 nm, which is well within the desired size range (<50 nm). For the population sampled, 89% of the particles were between 11 and 31 nm, with 56% having diameters between 19 and 24 nm. These particles are much better than Fe clusters obtained in solution phase using the methods of Zhang *et al.* [7], which had a bimodal size distribution around 300 and 640 nm (Figure 5). For selected samples, SEM photographs were also obtained of freeze-fractured cross sections to verify particle size both in the cross section and at the surface. These photographs (Figure 4) also showed a typical diameter of 20–30 nm. For the case of just Fe, EDX analysis of the particles was used to assess the purity of the Fe clusters. The qualitative results indicate that the reduced particles are Fe, with some boron and counterion impurities (that is, Cl, S). However, this type of analysis does not provide an indication of what state the Fe is in. Analysis of metal loss in the coagulation bath indicated an 11 ± 2% loss of Ni and 8 ± 1% loss of Fe during the synthesis process. Analysis of post-washing steps showed no detectable level of metals.

TCE Dechlorination Studies

For the TCE experiments, the average initial concentration for all runs was 9 ± 2 mg L^{-1} TCE. Using the small quantity of immobilized metal (31 mg total, Fe:

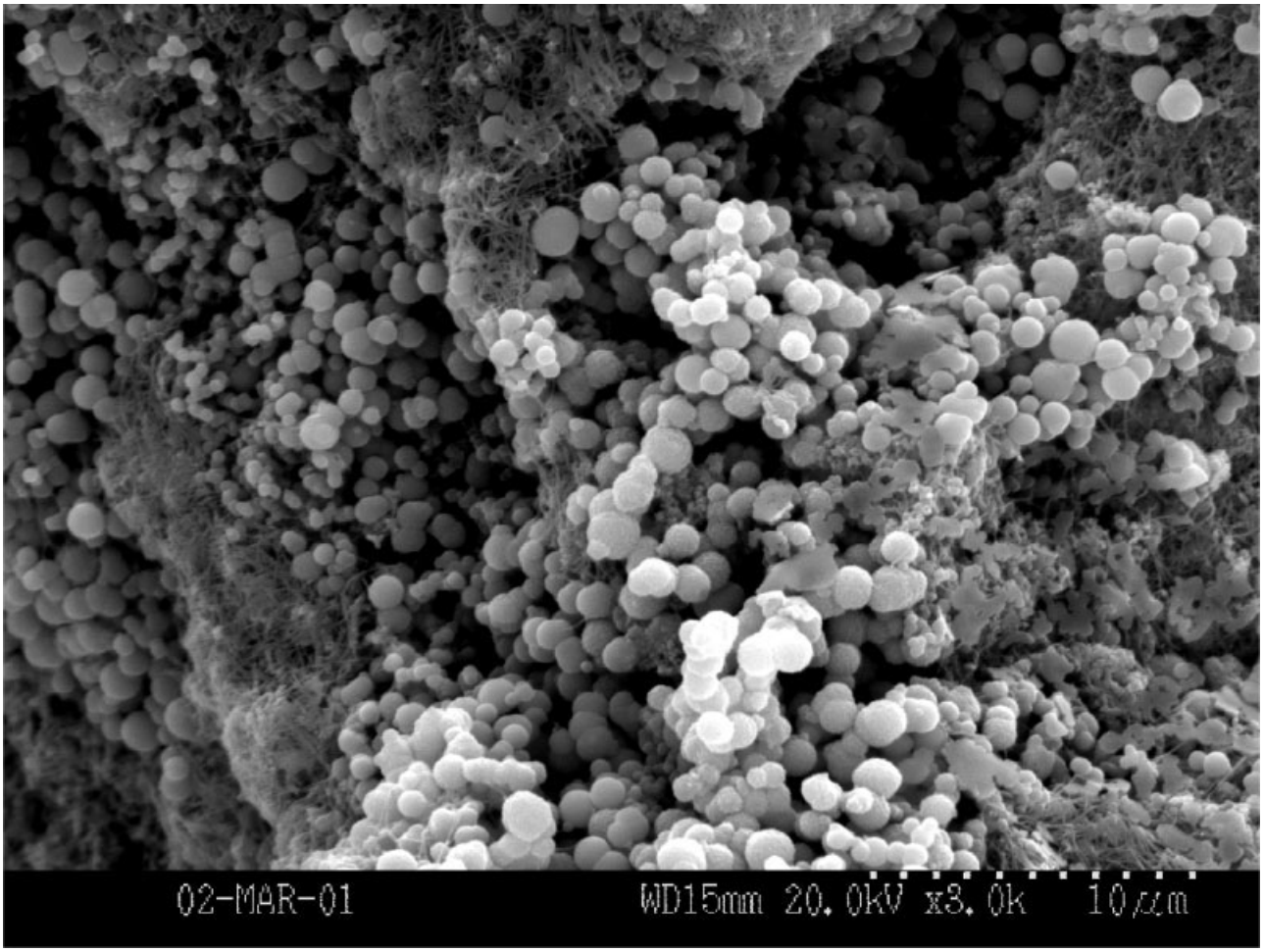

Figure 5. SEM picture of Fe clusters obtained during solution phase synthesis. The particles have a bimodal size distribution around diameters of 300 and 640 nm.

Ni = 4:1), it was possible to achieve a greater than 75% reduction in TCE levels in 4.25 h, with ethane as the only observable product. For shorter reaction times (<2 h), traces of *cis*- and *trans*-DCE could be extracted from the baseline of the MS chromatogram. For longer reaction times, products of coupling reactions (butane and hexane) were observed. This is consistent with findings reported in the literature by Arnold and Roberts [4] for Fe and Schrick *et al.* [15] for Fe/Ni. Analysis of metal loss shows that 0.5% of the total metals present (0.1 mg Fe and 0.05 mg Ni) in the film was leached out into the surrounding solution.

The time-dependent TCE destruction profile is shown in Figure 6. These data reflect changes in the total amount of TCE in the reactor (both the aqueous and membrane domain), and are expressed as the effective aqueous phase concentration. To obtain this value, the number of moles of TCE in the membrane was first calculated as the difference in moles of unreacted TCE as determined by PT-GC/MS and by pentane extraction. This value was then converted to a concentration by dividing it by the volume of solution in the reactor (0.11 L) and added to the aqueous phase TCE concentration to obtain the total effective concentration (C_u).

The kinetic data obtained for these seven experiments were fitted to a pseudo–first-order kinetic model with respect to the aqueous phase TCE concentration to obtain the governing reaction rate constant for the immobilized system. The resulting slope (observed rate constant) from a straight-line fit of $\ln(C_u/C_{u,0})$ vs. t (h) is 0.34 h^{-1} (R^2 = 0.92), where $C_{u,0}$ is the TCE concentration in the feed (Figure 5, inset). To compare this with available literature data, it is necessary to first calculate the surface-area–normalized rate constant (k_{SA}) as given in Eq. 3. Based on a 24-nm particle diameter, the available particle surface area per unit weight (a_s) is 32 $m^2\ g^{-1}$. For treatment of 110 mL of solution with 31 mg of metal, the mass loading in solution (ρ_m) is 0.28 $g\ L^{-1}$. The calculated surface area loading is 9.2 $m^2\ L^{-1}$. It is important to note that this is not necessarily the active surface area, which must be determined using chemisorption. Using this loading, the value of k_{SA} for the immobilized system is 3.7×10^{-2} $L\ m^{-2}\ h^{-1}$. This value is on the same order of magnitude as the value of 9.8×10^{-2} $L\ m^{-2}\ h^{-1}$ reported for aqueous phase bimetallic (Fe/Ni) dechlorination by Shrick *et al.* [15], involving 10- to 30-nm particles. However, this value is for a 3:1 (Fe:Ni) ratio. It is worth noting that the present results were obtained

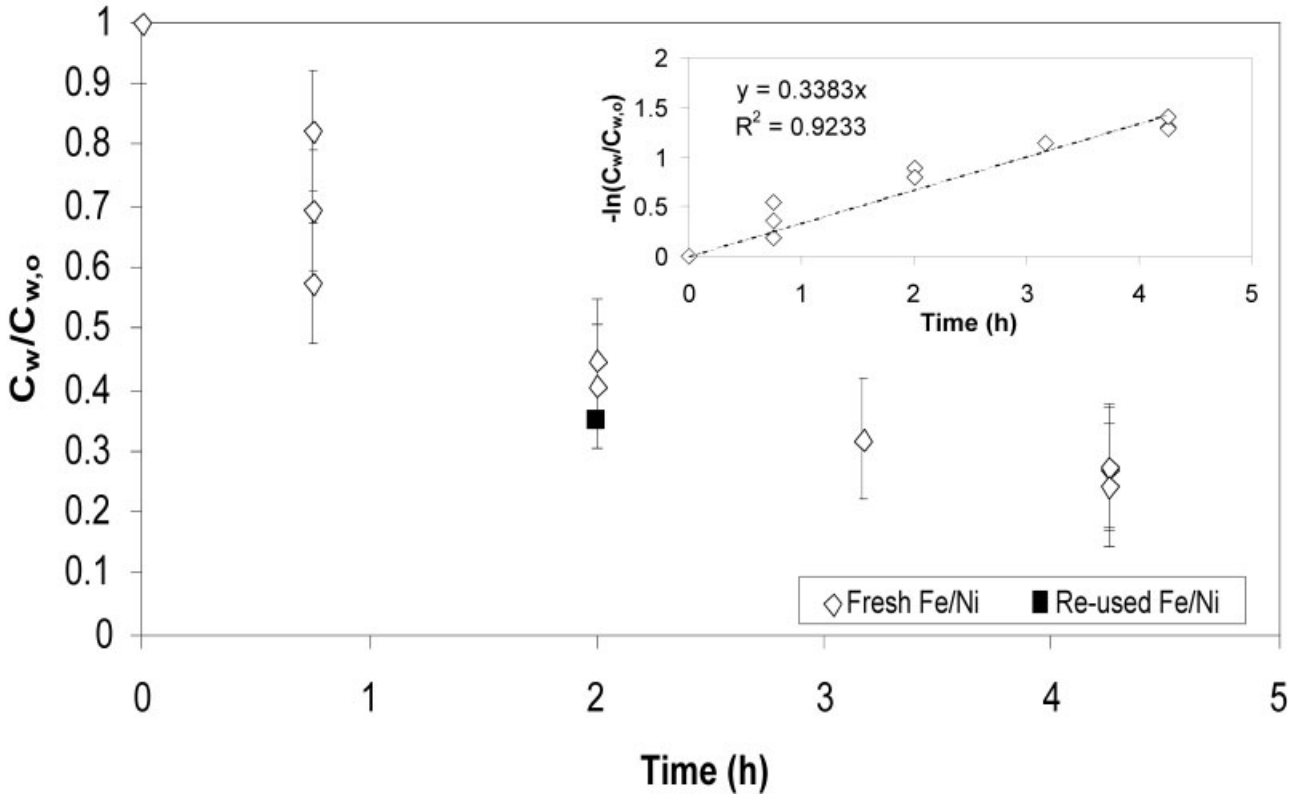

Figure 6. TCE destruction using 31 mg of Fe/Ni (Fe:Ni = 4:1) nanoparticles. Inset: The first-order linear fit of results to obtain the observed rate constant.

using approximately one tenth of the metal loading (g/L) used to obtain the literature results.

For the present work, we have accounted for mass transfer effects using data obtained from extraction of the membrane phase TCE to adjust the aqueous phase concentrations, reflecting the *actual* amount of unreacted TCE in the system. This is a key point of analysis when examining membrane-based systems. If the standard kinetic model (Eq. 2) is applied with no corrections, the resulting rate constant will not reflect the true kinetics of the system because it will not account for the TCE that is sorbed to the membrane. For example, the value of k_{SA} for our experiments, if sorption is not taken into account, is 6.7×10^{-2} L m^{-2} h^{-1}.

Dechlorination of DCE

To confirm that rapid dechlorination to ethane is possible, the destruction of *cis*-1,2-DCE, one of the first intermediates of TCE dehalogenation, was studied to determine whether its rate of reaction was faster than that of the parent compound. The results presented should be considered preliminary because they represent only single experiments for each time interval. The experiments involved films containing 32 mg of metal (Fe:Ni = 4:1) and an initial DCE concentration of 5 ± 2 mg L^{-1}. After 0.75 h, 82% of the DCE is removed, with a 91% removal by 1 h. Using first-order degradation behavior, the value of k_{SA} for these results is 2.7×10^{-1} L m^{-2} h^{-1}. This is an order of magnitude faster than TCE, which supports the hypothesis of rapid conversion of TCE to ethane after the initial dechlorination step. Studies by Arnold and Roberts [4] involving bulk Fe also showed that the reduction of TCE is the rate-controlling step.

Reusability of Materials

Further analysis of the films was performed to determine the reusability of the reactive metals in the film. During this experiment, a TCE solution was added to the reactor by spiking 110 mL of deoxygenated DIUF H_2O with a concentrated solution of TCE in methanol, to give a starting concentration of 9.5 mg L^{-1}. The reactor was placed on a shaker for 22.5 h to allow for complete reaction of the TCE. After obtaining aqueous samples, the reactor was respiked with the TCE-in-methanol solution and allowed to react for 2 h. Organic analysis of the reactor showed that a 65% reduction in TCE levels occurred after the respike. This result (shown as a solid point in Figure 6) is almost identical to the results of fresh membranes for a 2-h dechlorination period and suggests that the synthesized films should be capable of carrying out the destruction of TCE for much larger volumes of the organic solution. In fact, in the absence of unfavorable side reactions, this quantity (31 mg) of metal should be able to treat 1.5 L of solution. Using these results and the stoichiometry of Eq. 2 (3 mol Fe/mol TCE), 72% of the immobilized Fe is consumed for dechlorination. Thus, this system can offer a high efficiency in terms of metal usage. The presence of oxygen may affect this metal usage. In

addition, the membrane polymer may also play a role in minimizing the impact of dissolved oxygen by reducing iron hydroxide precipitate deposition on particles.

CONCLUSIONS

The present work has demonstrated the possibility of incorporating metallic nanoparticles in a polymeric film using the conventional phase-inversion synthesis technique for membrane fabrication. The cellulose acetate films were capable of stabilizing the growth of 24-nm particles with less than 8% loss of Fe and 11% loss of Ni during synthesis. When applied to dechlorination, the hybrid films demonstrated a greater than 75% reduction in TCE levels in 4.25 h using only a fraction (1/10) of the metal loading used in the literature. The resulting value of k_{SA} for the system indicates a substantial improvement over conventional aqueous phase dechlorination schemes using bulk-scale materials. The DCE dechlorination rate was about one order of magnitude higher than that of TCE, supporting previous findings that the first TCE degradation step is actually the rate-limiting step. Because various combinations of membranes containing immobilized metal nanoparticles can be achieved using the synthesis techniques presented, a more versatile application of zerovalent treatment is possible. A key benefit of this is that it can allow for potential minimization of side reactions by altering organic partitioning behavior.

ACKNOWLEDGMENTS

This work is made possible with funding provided by the U.S. EPA-STAR Program, NSF-IGERT, and NIEHS-SBRP programs. The authors thank Dr. Nora Savage of US EPA for providing valuable suggestions to this work. The contributions of K. Wood were done as an NSF/REU fellow.

LITERATURE CITED

1. Gillham, R.W., & O'Hannesin, S.F. (1994). Enhanced degradation of halogenated aliphatics by zero-valent iron, Ground Water, 32, 958–967.
2. Johnson, T.L., Scherer, M.M., & Tratnyek, P.G. (1996). Kinetics of halogenated organic compound degradation by iron metal, Environmental Science and Technology, 30, 2634–2640.
3. Choe, S., Lee, S., Chang, Y., Hwang, K., & Khim, J. (2001). Rapid reductive destruction of hazardous organic compounds by nanoscale Fe^0, Chemosphere, 42, 367–372.
4. Arnold, W.A., & Roberts, L.A. (2000). Pathways and kinetics of chlorinated ethylene and chlorinated acetylene reaction with Fe(0) particles, Environmental Science and Technology, 34, 1794–1805.
5. Arnold, W.A., & Roberts, A.L. (1998). Pathways of chlorinated ethylene and chlorinated acetylene reaction with Zn(0), Environmental Science and Technology, 32, 3017–3025.
6. Gotpagar, J.K., Grulke, E., Tsang, T., & Bhattacharyya, D. (1998). Reductive dehalogenation of trichloroethylene: kinetic models and experimental verification, Journal of Hazardous Materials, 62, 243–264.
7. Wang, B.W., & Zhang, W.X. (1997). Synthesizing nanoscale iron particles for rapid and complete dechlorination of TCE and PCBs, Environmental Science and Technology, 31, 2154–2156.
8. Su, C., & Puls, R.W. (1999). Kinetics of trichloroethene reduction by zero-valent iron and tin: pretreatment effect, apparent activation energy, and intermediate products, Environmental Science and Technology, 33, 163–168.
9. Burrow, P.D., Kayvan, A., & Gallup, G.A. (2000). Dechlorination rate constants on iron and the correlation with electron attachment energies, Environmental Science and Technology, 34, 3368–3371.
10. Farrell, J., Kason, M., Melitas, N., & Li, T. (2000). Investigation of the long-term performance of zerovalent iron for reductive dechlorination of trichloroethylene, Environmental Science and Technology, 34, 514–521.
11. Wust, W.F., Kober, R., Schlicker, O., & Dahmke, A. (1999). Combined zero- and first-order kinetic model of the degradation of TCE and *cis*-DCE with commercial iron, Environmental Science and Technology, 33, 4304–4309.
12. Boronina, T.N.,; Lagadic, I., Sergeev, G.B., & Klabunde, K.J. (1998). Activated and nonactivated forms of zinc powder: reactivity toward chlorocarbons in water and AFM studies of surface morphologies, Environmental Science and Technology, 32, 2614–2622.
13. Tratnyek, P.G., Scherer, M.M., Deng, B., & Hu, S. (2001). Effects of natural organic matter, anthropogenic surfactants, and model quinones on the reduction of contaminants by zero-valent iron, Water Research, 35, 4435–4443.
14. Zhang, W., Wang, C., & Lien, H. (1998). Treatment of chlorinated organic contaminants with nanoscale bimetallic particles, Catalysis Today, 40, 387–395.
15. Schrick, B., Blough, J., Jones, A., & Mallouk, T. (2002). Hydrodechlorination of trichloroethylene to hydrocarbons using bimetallic nickel-iron nanoparticles, Chemistry of Materials, 14, 5140–5147.
16. Gotpagar, J.K., Grulke, E., Tsang, T., & Bhattacharyya, D. (1999). Reductive dehalogenation of trichloroethylene with zero-valent iron: surface profiling microscopy and rate enhancement studies, Langmuir, 15, 8412–8420.
17. Zhang, W. (2003). Nanoscale iron particles for environmental remediation: an overview, Journal of Nanoparticle Research, 5, 323–332.
18. Zhang, W., & Masciangioli, T. (2003). Environmental technologies at the nanoscales, Environmental Science and Technology, 37, 102A–108A.
19. Xu, Y., & Zhang, W. (2000). Subcolloidal Fe/Ag particles for reductive dehalogenation of chlorinated benzenes, Industrial and Engineering Chemistry Research, 39, 2238–2244.
20. Ponder, S.M., Darab, J., Bucher, J., Caulder, D., Craig, I., Davis, L., Edelstein, N., Lukens, W., Nitsche, H., Rao, L., Shuh, D., & Mallouk, T. (2001). Surface chemistry and electrochemistry of supported zerovalent iron nanoparticles in the reme-

diation of aqueous metal contaminants, Chemistry of Materials, 13, 479–486.
21. Glavee, G.N., Klabunde, K.J., Sorenson, C.M., & Hadjipanayis, G.C. (1995). Chemistry of borohydride reduction of iron (II) and iron (III) ions in aqueous and nonaqueous media. Formation of nanoscale Fe, FeB, and Fe_2B powders, Inorganic Chemistry, 34, 28–35.
22. Calvin, S., Carpenter, E.E., & Harris, V.G. (2003). Characterization of passivated iron nanoparticles by X-ray absorption spectroscopy, Physical Review B: Condensed Matter and Materials Physics, 68, 033411/1–033411/4.
23. Sato, H., Ohtsu, T., & Komasawa, I. (2000). Atomic force microscopy study of ultrafine particles prepared in reverse micelles, Journal of Colloid and Interface Science, 230, 200–204.
24. Carpenter, E., Seip, C., & O'Connor, C. (1999). Magnetism of nanophase metal and metal alloy particles formed in ordered phases, Journal of Applied Physics, 85, 5184–5186.
25. Sidrov, S.N., Bronstein, L.M., Davankov, V.A., Tsyurupa, M.P., Solodovnikov, S.P., Valetsky, P.M., Wilder, E.A., & Spontak, R.J. (1999). Cobalt nanoparticle formation in the pores of hyper-crosslinked polystyrene: control of nanoparticle growth and Morphology, Chemistry of Materials, 11, 3210–3215.
26. Tannenbaum, R. (1998). Metal cluster growth limited by polymer surface interactions, Current Trends in Polymer Science, 3, 81–98.
27. Hashimoto, T., Kiyoharu, T., & Funaki, Y. (1997). Nanoprocessing based on bicontinuous microdomains of block copolymers: nanochannels coated with metals, Langmuir, 13, 6869–6872.
28. Tsutsumi, K., Funaki, Y., Hirokawa, Y., & Hashimoto, T. (1999). Selective incorporation of palladium nanoparticles into microphase-separated domains of poly(2-vinylpyridine)-block-polyisoprene, Langmuir, 15, 5200–5203.
29. Williams, M.E., Hestekin, J.A., Smothers, C.N., & Bhattacharyya, D. (1999). Separation of organic pollutants by reverse osmosis and nanofiltration membranes: mathematical models and experimental verification, Industrial and Engineering Chemistry Research, 38, 3683–3695.
30. Ho, W.S., & Sirkar, K. (Eds.) (1992). The membrane handbook, New York: Van Nostrand Reinhold.
31. Sourirajan, S., & Matsuura, T. (1985). Reverse osmosis/ultrafiltration process principles (p. 458), Ottawa: National Research Council Canada.
32. Chen, J., Al-Abed, S., Ryan, J., & Li, Z. (2001). Effects of pH on dechlorination of trichloroethylene by zero-valent iron, Journal of Hazardous Materials, 83, 243–254.
33. Ritter, K., Odziemkowski, M., Simpgraga, R., Gillham, R., & Irish, D. (2003). An in situ study of the effect of nitrate on the reduction of trichloroethylene by granular iron, Journal of Contaminant Hydrology, 65, 121–136.
34. Arnold, W.A., Winget, P., & Cramer, C.J. (2002). Reductive dechlorination of 1,1,2,2-tetrachloroethane, Environmental Science and Technology, 36, 3536–3541.